

***Boerhavia diffusa* (Punarnava) Root Extract as Green Corrosion Inhibitor for Mild Steel in Hydrochloric Acid Solution: Theoretical and Electrochemical studies**

Ambrish Singh¹, Eno. E. Ebenso², M. A. Quraishi^{1*}

¹ Department of Applied Chemistry, Institute of Technology, Banaras Hindu University, Varanasi 221 005 (India)

² Department of Chemistry, North-West University (Mafikeng Campus), Mmabatho 2735, South Africa

*E-mail: maqraishi.apc@itbhu.ac.in

Received: 8 July 2012 / Accepted: 14 August 2012 / Published: 1 September 2012

The effect of extract of Punarnava (*Boerhavia diffusa*) on corrosion of mild steel was investigated by gravimetric, potentiodynamic polarization, electrochemical impedance spectroscopy. Tafel polarization results revealed that the maximum displacement of $-E_{corr}$ value is 46 mV hence the extract acted as mixed-type inhibitor. The inhibition efficiency increases up to 96% at 300 ppm and decreases with increase in the temperature. The charge transfer resistance (R_{ct}) value of inhibited system increased from $68 \Omega \text{ cm}^2$ to $426 \Omega \text{ cm}^2$ and double layer capacitance (C_{dl}) value decreased from $37 \mu\text{Fcm}^{-2}$ to $17 \mu\text{Fcm}^{-2}$ with increasing inhibitor concentration. Langmuir adsorption isotherm was followed by the inhibitor molecules on steel surface. The low value of energy gap (ΔE) further provided support for high efficiency of the extract.

Keywords: Mild steel; EIS; Acid corrosion; Quantum calculations

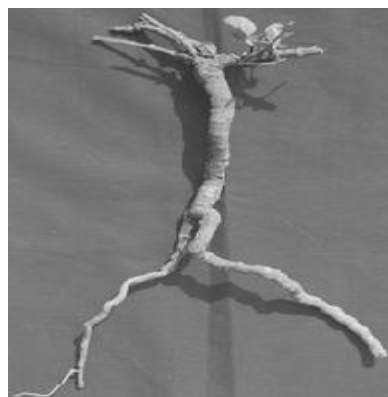
1. INTRODUCTION

The known hazardous effect of most synthetic corrosion inhibitors has motivated scientists to use natural products as corrosion inhibitors as they are inexpensive, readily available and renewable sources of materials, environmentally friendly and ecologically acceptable.

Compounds that contain π -bonds generally exhibit good inhibitive properties by supplying electrons via the heteroatoms (N, S or O). Plant extracts has been reported as green corrosion inhibitors by several authors [1-15]. It is reported in literature that the root of *B. diffusa* contains alkaloids

(punarnavine), rotenoids (boeravinones B-H), flavonoids, amino acids, lignans (liriodendrons), β -sitosterols and tetracosanoic, esacosanoic, stearic and ursolic acids. Figure 1 shows the structures of some active constituents of *B. diffusa*. The root of *B. diffusa* is used for the treatment of many diseases, such as liver disorders (jaundice, hepatitis, etc.), gastro-intestinal disorders (as laxative), renal disorders (for calculations, cystitis and nephritis), and for the treatment of anaemia and of menstrual syndrome. The drug has recently been used as an adjuvant in an anticancer therapy [16-18].

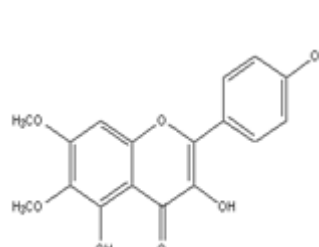
The gravimetric and electrochemical techniques were used to study the extract. The effect of temperature on the corrosion behaviour of steel in the absence and presence of the extract was also studied.



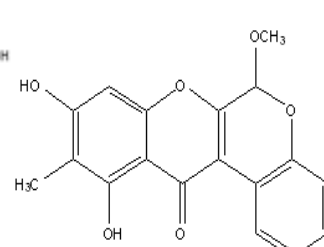
Punarnava root



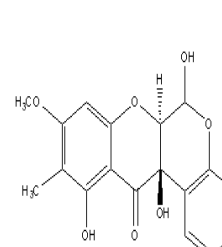
Punarnava Dried roots



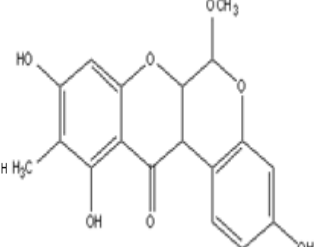
Eupalitin



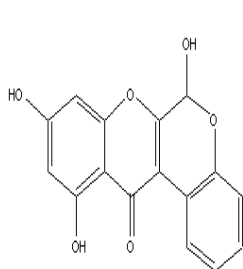
Boeravinone B



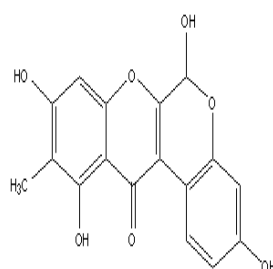
Boeravinone C



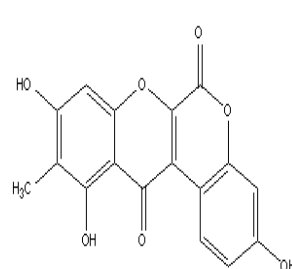
Boeravinone D



Coccineone B



Coccineone E



Boeravinone F

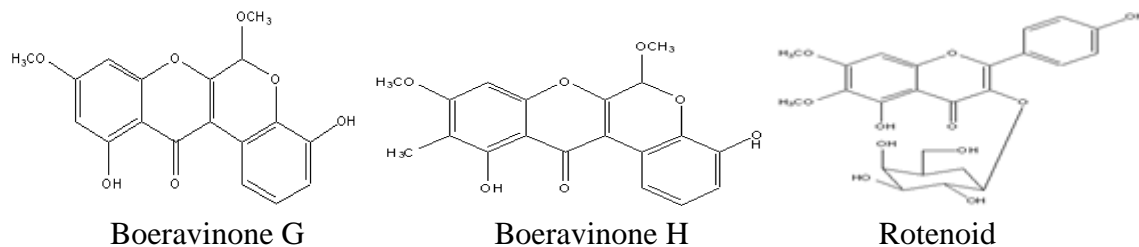


Figure 1. Structure of active constituents of Punarnava (*Boerhavia diffusa*) extract

2. EXPERIMENTAL

2.1 Inhibitor

Stock solutions of Punarnava (*Boerhavia diffusa*) dried powder (10 g) was soaked in double distilled water (500 mL) and refluxed for 5 h. The aqueous solution was filtered and concentrated to 100 mL. This extract was used to study the corrosion inhibition properties. Corrosion tests were performed on a mild steel of the following percentage composition: Fe 99.30%, C 0.076%, Si 0.026%, Mn 0.192%, P 0.012%, Cr 0.050%, Ni 0.050%, Al 0.023%, and Cu 0.135%. Prior to all measurements, the mild steel specimens were abraded successively with Emery papers from 600 to 1200 grades. The specimens were washed thoroughly with double distilled water, degreased with acetone and finally dried in hot air blower. And then, the specimens were placed in the desiccator for backup. The aggressive solution of 1 M HCl was prepared by dilution of analytical grade HCl (37%) with double distilled water and all experiments were carried out in unstirred solutions. The rectangular specimens with dimension $2.5 \times 2.0 \times 0.025$ cm³ were used in weight loss experiments and of size 1.0×1.0 cm² (exposed) with a 7.5 cm long stem (isolated with commercially available lacquer) were used for electrochemical measurements.

2.2. Weight loss method

Weight loss measurements were performed on rectangular mild steel samples having size $2.5 \times 2.0 \times 0.025$ cm³ by immersing the mild steel coupons into acid solution (100 mL) in absence and presence of different concentrations of Punarnava (*Boerhavia diffusa*) extract. After the elapsed time, the specimen were taken out, washed, dried and weighed accurately. All the tests were conducted in aerated 1 M HCl. All the experiments were performed in triplicate and average values were reported. The inhibition efficiency (η %) and surface coverage (θ) was determined by using following equation:

$$\theta = \frac{w_o - w_i}{w_o} \quad (1)$$

$$\eta\% = \frac{w_o - w_i}{w_o} \times 100 \quad (2)$$

where w_i and w_0 are the weight loss values in presence and absence of inhibitor, respectively.

The corrosion rate (C_R) of mild steel was calculated using the relation:

$$C_R (\text{mmy}^{-1}) = \frac{87.6 \times w}{AtD} \quad (3)$$

where w is weight loss of mild steel (mg), A the area of the coupon (cm^2), t is the exposure time (h) and D the density of mild steel (g cm^{-3}).

2.3 Electrochemical impedance spectroscopy

The EIS tests were performed at 308 K in a three electrode assembly. A saturated calomel electrode was used as the reference; a 1 cm^2 platinum foil was used as counter electrode. All potentials were reported versus SCE. Electrochemical impedance spectroscopy measurements (EIS) were performed using a Gamry instrument Potentiostat/Galvanostat with a Gamry framework system based on ESA 400 in a frequency range of 10^{-2} Hz to 10^5 Hz under potentiodynamic conditions, with amplitude of 10 mV peak-to-peak, using AC signal at E_{corr} . Gamry applications include software DC105 for corrosion and EIS300 for EIS measurements, and Echem Analyst version 5.50 software packages for data fitting. The experiments were carried out after 30 min. of immersion in the testing solution (no deaeration, no stirring).

The inhibition efficiency of the inhibitor was calculated from the charge transfer resistance values using the following equation:

$$\mu\% = \frac{R_{\text{ct}}^{\text{i}} - R_{\text{ct}}^0}{R_{\text{ct}}^{\text{i}}} \times 100 \quad (4)$$

where, R_{ct}^0 and R_{ct}^{i} are the charge transfer resistance in absence and in presence of inhibitor, respectively.

2.4 Potentiodynamic polarization

The electrochemical behaviour of mild steel sample in inhibited and uninhibited solution was studied by recording anodic and cathodic potentiodynamic polarization curves. Measurements were performed in the 1 M HCl solution containing different concentrations of the tested inhibitor by changing the electrode potential automatically from -250 to +250 mV versus corrosion potential at a scan rate of 1 mV S⁻¹. The linear Tafel segments of anodic and cathodic curves were extrapolated to corrosion potential to obtain corrosion current densities (i_{corr}). From the polarization curves obtained, the corrosion current (i_{corr}) was calculated by curve fitting using the equation:

$$I = i_{\text{corr}} \left[\exp\left(\frac{2.3\Delta E}{b_a}\right) - \exp\left(-\frac{2.3\Delta E}{b_c}\right) \right] \quad (5)$$

The inhibition efficiency was evaluated from the measured i_{corr} values using the relationship:

$$\mu\% = \frac{i_{\text{corr}}^0 - i_{\text{corr}}^i}{i_{\text{corr}}^0} \times 100 \quad (6)$$

where, i_{corr}^0 and i_{corr}^i are the corrosion current density in absence and presence of inhibitor, respectively.

2.5 Linear polarization measurement

The corrosion behaviour was studied with polarization resistance measurements (R_p) in 1 M HCl solution with and without different concentrations of studied inhibitor. The linear polarization study was carried out from cathodic potential of -20 mV versus OCP to an anodic potential of + 20 mV versus OCP at a scan rate 0.125 mV S⁻¹ to study the polarization resistance (R_p) and the polarization resistance was evaluated from the slope of curve in the vicinity of corrosion potential. From the evaluated polarization resistance value, the inhibition efficiency was calculated using the relationship:

$$\mu\% = \frac{R_p^i - R_p^0}{R_p^i} \times 100 \quad (7)$$

where, R_p^0 and R_p^i are the polarization resistance in absence and presence of inhibitor, respectively.

2.6. Theoretical study

All the calculations were performed with Gaussian 03 for windows. The molecular structures of the neutral species were fully and geometrically optimized using the functional hybrid B3LYP (Becke, three-parameter, Lee-Yang-Parr exchange-correlation function) Density function theory (DFT) formalism with electron basis set 6-31G (*, *) for all atoms. The quantum chemical parameters obtained were HOMO, LUMO, ΔE LUMO-HOMO, dipole moment and Molecular volume [19].

3. RESULTS AND DISCUSSION

3.1 Electrochemical impedance spectroscopy

Impedance spectra for mild steel in 1 M HCl in absence and presence of different concentrations of extract are shown in the form of Nyquist plots (Fig. 2a). It followed from Fig. 2a that the impedance of the inhibited mild steel increases with increase in the inhibitor concentration and consequently the inhibition efficiency also increases. A depressed semicircle is mostly referred to as frequency dispersion which could be attributed to different physical phenomena such as roughness and inhomogeneities of the solid surfaces, impurities, grain boundaries and distribution of the surface active sites [20]. The fact that this semicircle cannot be observed after the addition of higher concentration supports our view [21, 22].

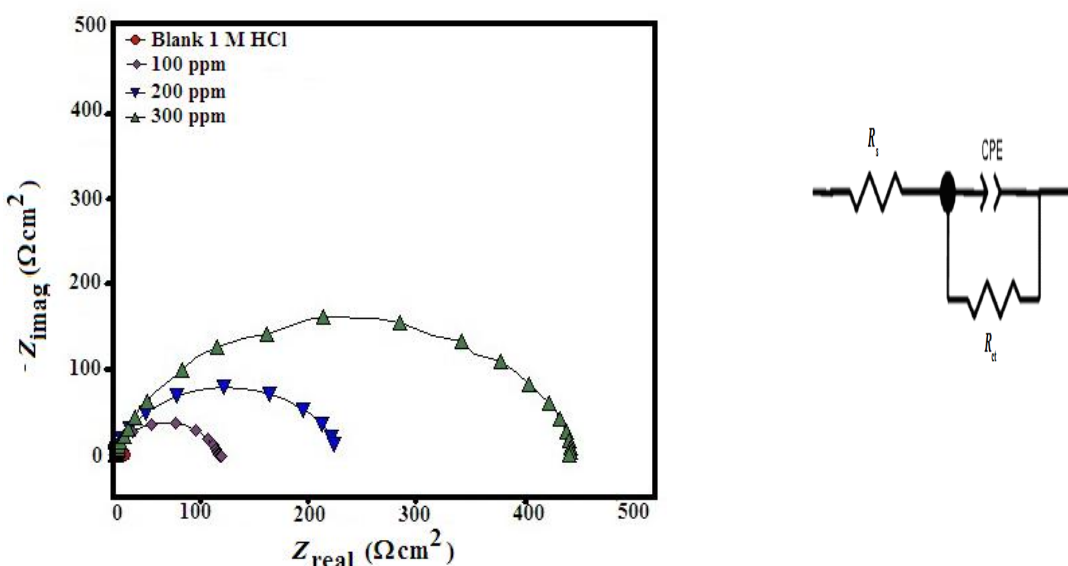


Figure 2. (a) Nyquist plots of mild steel in 1 M HCl in absence and presence of different concentrations of Punarnava (*Boerhavia diffusa*) extract (b) equivalent circuit used to fit the impedance data

Different corrosion parameters derived from EIS measurements are presented as Table 1. It is shown from Table 1 that R_{ct} of inhibited system increased from $68 \Omega\text{cm}^2$ to $426 \Omega\text{cm}^2$ and double layer capacitance C_{dl} decreased from $37 \mu\text{Fcm}^{-2}$ to $17 \mu\text{Fcm}^{-2}$ with increasing inhibitor concentration. This decrease in C_{dl} results from a decrease in local dielectric constant and/or an increase in the thickness of the double layer, suggested that inhibitor molecules inhibit the iron corrosion by adsorption at the metal/acid interface.

To get more accurate fit of these experimental data, the measured impedance data were analyzed by fitting in to equivalent circuit given in Fig. 2b. Excellent fit with this model was obtained for all experimental data.

Mathematically, amplitude of CPE is given by the relation:

$$Z_{\text{CPE}} = Q^{-1} (j\omega)^{-n} \quad (8)$$

where Q is the magnitude of the CPE, j is the imaginary unit, ω is the angular frequency ($\omega = 2\pi f$, the frequency in Hz), and n is the phase shift which gives details about the degree of surface inhomogeneity. When $n = 1$, this is the same equation as that for the impedance of a capacitor, where $Q = C_{\text{dl}}$. In fact, when n is close to 1, the CPE resembles a capacitor, but the phase angle is not 90° . It is constant and somewhat less than 90° at all frequencies.

The electrochemical parameters are listed in Table 1. C_{dl} values derived from CPE parameters are listed in Table 1. For providing simple comparison between the capacitive behaviors of different corrosion systems, the values of Q were converted to C_{dl} using the relation [23]:

$$C_{\text{dl}} = Q(\omega_{\text{max}})^{n-1} \quad (9)$$

where, ω_{max} represents the frequency at which the imaginary component reaches a maximum. It is the frequency at which the real part (Z_r) is midway between the low and high frequency x-axis intercepts.

Table 1. Calculated electrochemical parameters for mild steel in absence and presence of different concentrations of Punarnava (*Boerhavia diffusa*) extract

Inhibitor	Conc. (ppm)	Tafel data				Linear polarization data				EIS data				
		$-E_{\text{corr}}$ (mV vs. SCE)	i_{corr} ($\mu\text{A cm}^{-2}$)	β_a (mV d^{-1})	β_c (mV d^{-1})	μ %	R_p ($\Omega \text{ cm}^2$)	μ %	R_s (Ω cm^2)	Q ($\Omega^{-1} \text{ sn}$ cm^2)	n	R_{ct} (Ω cm^2)	C_{dl} (μF cm^{-2})	μ %
Blank	446	1540	90	121	-	8	-	1.20	250	0.827	8	69	-	
Punarnava (<i>Boerhavia diffusa</i>) extract	100	469	382	94	119	75	42	80	1.33	57	0.823	68	37	88
	200	480	131	65	86	91	98	91	1.59	41	0.871	209	29	96
	300	492	67	44	59	95	255	96	1.81	27	0.889	426	17	98

3.2 Potentiodynamic Polarization

The Tafel polarization curves of mild steel in hydrochloric acid solution, in the absence and presence of different concentrations of Punarnava (*Boerhavia diffusa*) extract, are presented in Fig. 3 and listed in Table 1. The maximum inhibition efficiency (95%) was obtained at a concentration of 300 ppm.

Addition of the Punarnava (*Boerhavia diffusa*) extract to acid media affected both the cathodic and anodic parts of the curves. For the inhibited system, if the displacement in $-E_{\text{corr}}$ value is greater than 85 mV relative to uninhibited system than the inhibitor is classified as cathodic or anodic type. In our case, the maximum displacement of $-E_{\text{corr}}$ value is 46 mV, hence the Punarnava (*Boerhavia diffusa*) extract is classified as a mixed-type inhibitor. The inhibition efficiency values in the Table 1 showed that the Punarnava (*Boerhavia diffusa*) extract acted as very effective corrosion inhibitor for mild steel in HCl solution and its capacity of inhibition increased with increase of concentration.

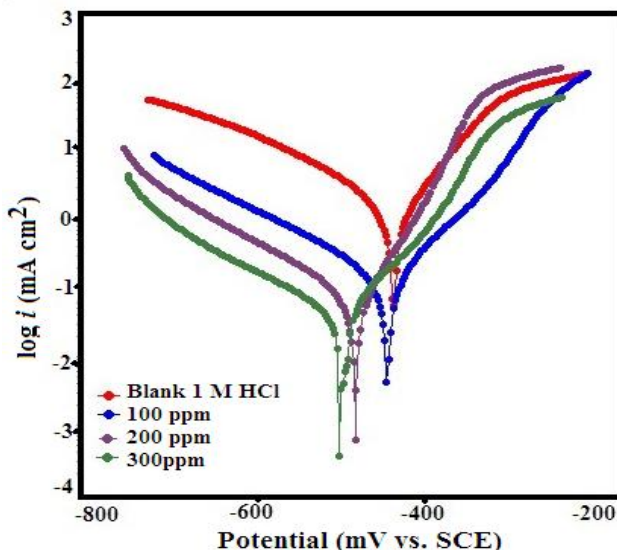


Figure 3. Tafel polarization curves for corrosion of mild steel in 1 M HCl in the absence and presence of different concentrations of Punarnava (*Boerhavia diffusa*) extract

3.3 Linear polarization measurement

The inhibition efficiencies and polarization resistance parameters are presented in Table 1. The linear polarization values increased from $42 \Omega \text{ cm}^2$ to $255 \Omega \text{ cm}^2$ resulting in a high inhibition efficiency of 96% at 300 ppm. The results obtained from Tafel polarization and EIS showed good agreement with the results obtained from linear polarization resistance.

3.4 Weight loss measurements

3.4.1 Effect of inhibitor concentration

The effect of inhibitor concentration on inhibition efficiency of steel in 1 M HCl was examined. Maximum inhibition efficiency of 96% was shown at 300 ppm in HCl solution. The values of percentage inhibition efficiency ($\eta\%$) and corrosion rate (C_R) obtained from weight loss method at different concentrations of Punarnava (*Boerhavia diffusa*) extract at 308 K are summarized in Table 2.

Table 2. Corrosion rate and Inhibition efficiency values for the corrosion of mild steel in 1 M HCl in the absence and presence of different concentrations of Punarnava (*Boerhavia diffusa*) extract from weight loss measurements at 308 K

Name of Inhibitor	Concentration of Inhibitor (ppm)	Surface Coverage (θ)	η %	$C_R (\text{mmy}^{-1})$
1 M HCl	-	-	-	77
<i>Boerhavia diffusa</i> (Punarnava) extract	50	0.73	73	21
	100	0.89	89	8
	200	0.93	93	5
	300	0.96	96	3

3.4.2 Effect of temperature

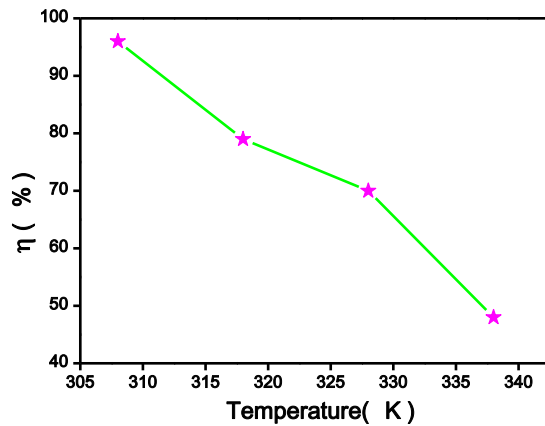


Figure 4. Inhibition efficiency of Punarnava (*Boerhavia diffusa*) extract at different temperatures

In order to investigate the effect of temperature on the performance of studied inhibitor and to derive thermodynamic activation and adsorption parameters, weight loss studies were performed at four different temperatures as depicted in Figure 4. The inhibition efficiency of Punarnava (*Boerhavia diffusa*) extract decreases with increasing temperature.

3.4.3 Thermodynamic activation parameters

The dependence of corrosion rate at temperature can be expressed by Arrhenius equation and transition state equation:

$$\log(C_R) = \frac{-E_a}{2.303RT} + \log \lambda \quad (10)$$

$$C_R = \frac{RT}{Nh} \exp\left(\frac{\Delta S^*}{R}\right) \exp\left(-\frac{\Delta H^*}{RT}\right) \quad (11)$$

where E_a apparent activation energy, λ the pre-exponential factor, ΔH^* the apparent enthalpy of activation, ΔS^* the apparent entropy of activation, h Planck's constant and N the Avogadro number.

The apparent activation energy for Punarnava (*Boerhavia diffusa*) extract is presented in Table 3. As it can be seen from Table 3, the values of activation free energy of Punarnava (*Boerhavia diffusa*) extract are higher than that of free acid solution. Thus, the corrosion rate of mild steel is mainly controlled by activation parameters.

The linear regression between $\log(C_R)$ vs. $1/T$ (Figure 5a) and $\log(C_R/T)$ vs. $1/T$ (Figure 5b) were performed. Straight lines obtained with a slope $(-\Delta E_a/2.303R)$, $(-\Delta H^*/2.303R)$ and an intercept of $[\log(R/Nh) + (\Delta S^*/2.303R)]$, from which the value of E_a , ΔH^* and ΔS^* were calculated and presented in Table 3.

Table 3. Thermodynamic parameters for the adsorption of Punarnava (*Boerhavia diffusa*) extract in 1 M HCl on the mild steel

Inhibitor conc. (ppm)	E_a (kJ mol ⁻¹)	A	$-\Delta H^*$ (kJ mol ⁻¹)	ΔS^* (kJ mol ⁻¹)
1 M HCl	29	1.23 E+7	22	-137
300 ppm (in HCl)	67	8.93 E+10	54	-37

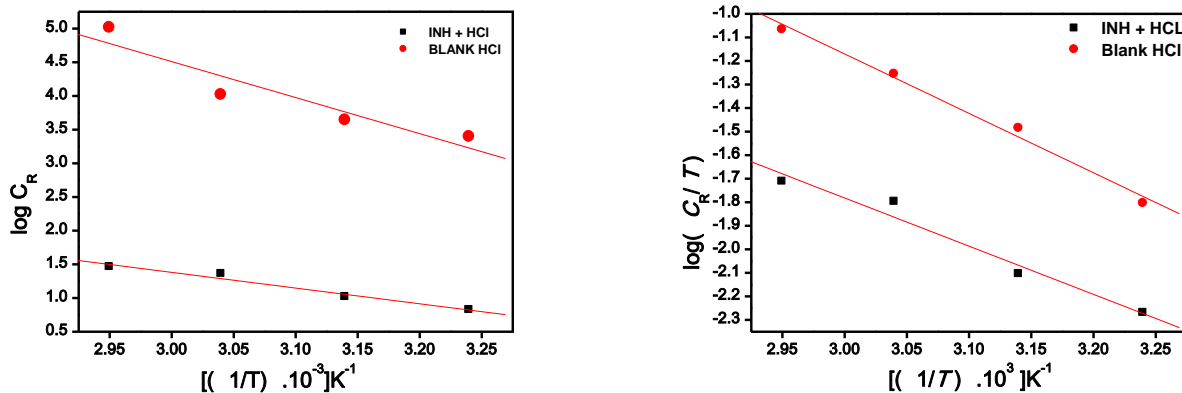
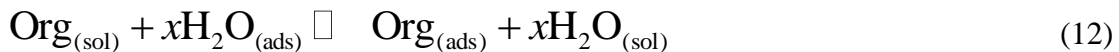


Figure 5. Arrhenius plots for (a) $\log C_R$ versus $1/T$ (b) $\log(C_R/T)$ versus $1/T$

3.4.4 Thermodynamic parameters and adsorption isotherm

The efficiency of Punarnava (*Boerhavia diffusa*) extract molecules as a successful corrosion inhibitor mainly depends on their adsorption ability on the metal surface. To emphasize the nature of adsorption, the adsorption of an organic adsorbate at metal/solution interface can be presented as a substitution adsorption process between the organic molecules in aqueous solution $\text{Org}_{(\text{sol})}$, and the water molecules on metallic surface H_2O [24]:



where, x is the size ratio representing the number of water molecules replaced by one molecule of organic adsorbate, $\text{Org}_{(\text{sol})}$ and $\text{Org}_{(\text{ads})}$ are the organic molecules in the solution and adsorbed on the metal surface, respectively. It is essential to know the mode of adsorption and the

adsorption isotherm that can give important information on the interaction of inhibitor and metal surface. Attempts were made to fit surface coverage values determined from weight loss measurements into different adsorption isotherm models. The linear regression coefficient values (R^2) determined from the plotted curve was found to be in the range of 0.9993 for Langmuir.

Langmuir adsorption isotherm can be expressed by following equation:

$$\frac{C_{(\text{inh})}}{\theta} = \frac{1}{K_{(\text{ads})}} + C_{(\text{inh})} \quad (13)$$

where, C_{inh} is inhibitor concentration and K_{ads} is an equilibrium constant for adsorption-desorption process.

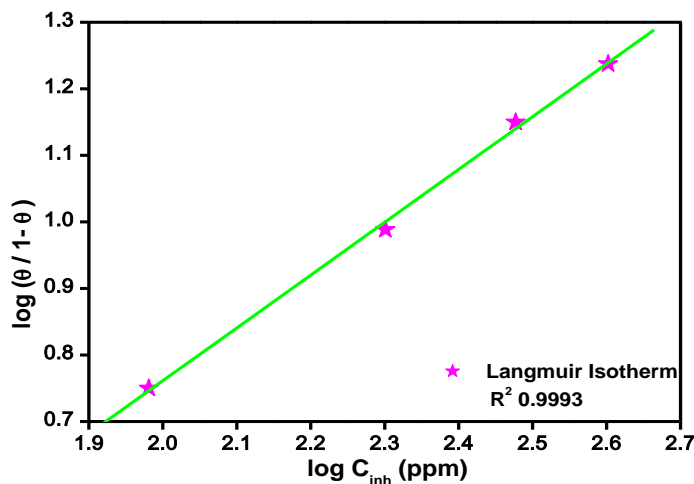
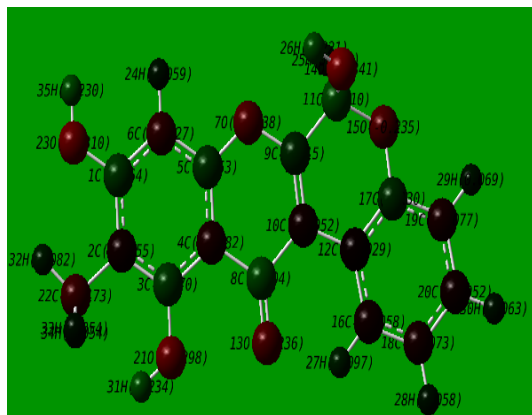


Figure 6. Langmuir adsorption isotherm plot for the adsorption of Punarnava (*Boerhavia diffusa*) extract on the surface of mild steel

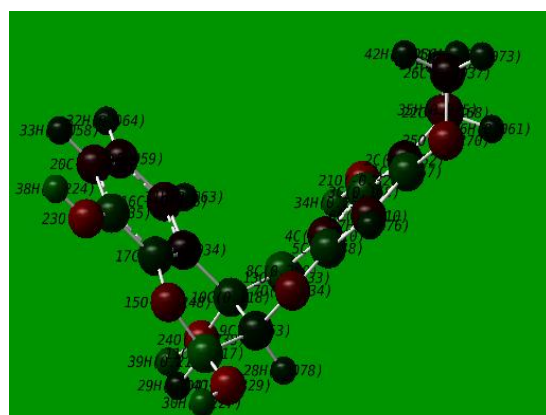
3.6. Quantum Chemical Calculations

Quantum chemical calculations were carried out in order to investigate adsorption and inhibition mechanism of various inhibitor molecules in the extract [25]. Figure 8 show full geometry optimization of the inhibitor molecules with Mulliken charges. The Frontier molecular orbital (FMO) density distributions of the inhibitor molecules present in Punarnava (*Boerhavia diffusa*) extract are shown in Figure 8 (a-b). Frontier orbital theory is useful in predicting adsorption centers of the inhibitor molecules responsible for the interaction with surface atoms. Excellent corrosion inhibitors are usually those compounds who not only offer electrons to unoccupied orbital of the metal, but also accept free electrons from the metal. It is important to focus on the parameters that directly influence the electronic interaction of the inhibitor molecules with the metal surface. These are mainly: E_{HOMO} , E_{LUMO} , ΔE ($E_{\text{LUMO}} - E_{\text{HOMO}}$), and dipole moment μ . The values of calculated quantum chemical parameters such as E_{HOMO} , E_{LUMO} , ΔE ($E_{\text{LUMO}} - E_{\text{HOMO}}$) and μ of Punarnava (*Boerhavia diffusa*) extract are listed in Table 4. Molecular volume was also calculated with the help of Chembio 3D Ultra 12.0

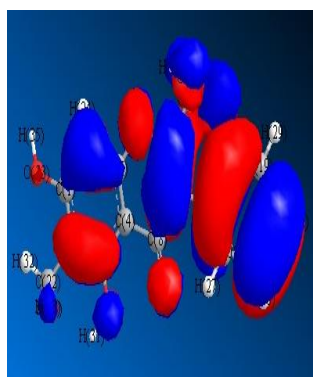
and Gaussian 03 W. E_{HOMO} is always associated with the electron donating ability of the molecule; high values of E_{HOMO} are likely to indicate a tendency of the molecule to donate electrons to appropriate acceptor molecules with low-energy orbital. Higher values of the E_{HOMO} facilitate adsorption (and therefore inhibition) by influencing the transport process through the adsorbed layer. Therefore, the energy of the E_{LUMO} indicates the ability of the molecule to accept electrons; hence these are the acceptor states.



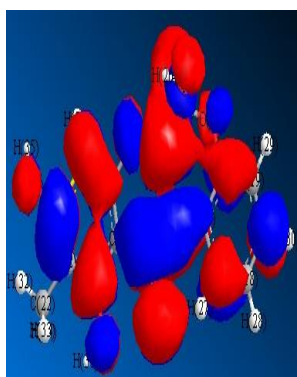
Boeravinone B Optimized



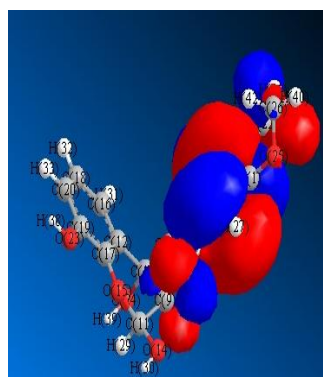
Boeravinone C Optimised



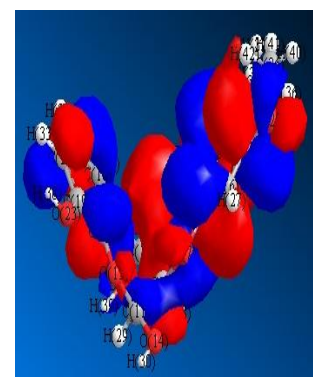
Boeravinone B HOMO Boeravinone B LUMO Boeravinone C HOMO



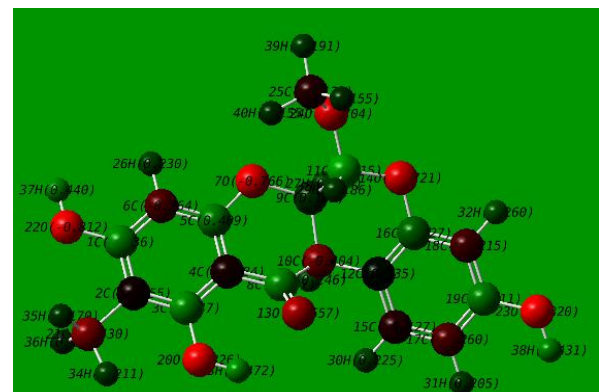
Boeravinone B LUMO



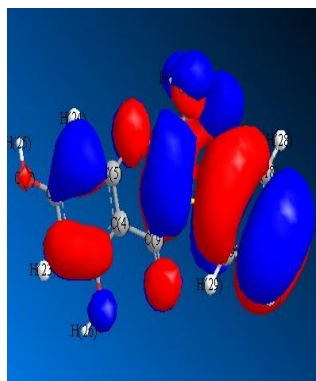
Boeravinone C LUMO



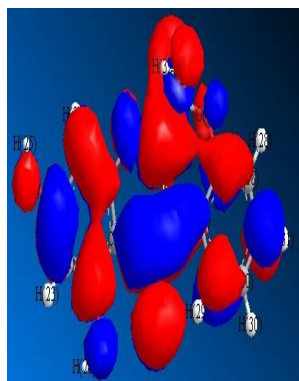
Coccineone B Optimised



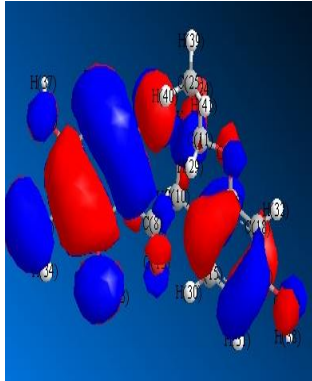
Boeravinone D Optimised



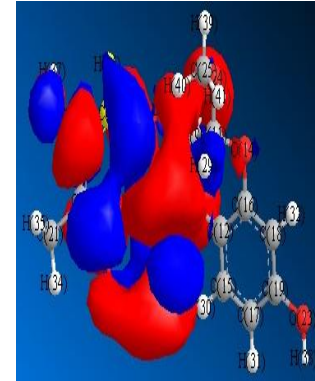
Coccineone B Homo



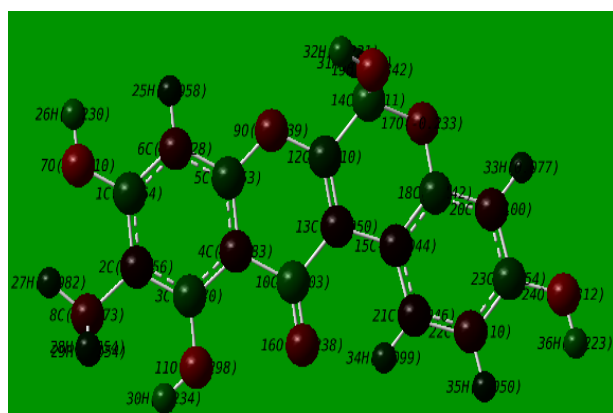
Coccineone B Lumo



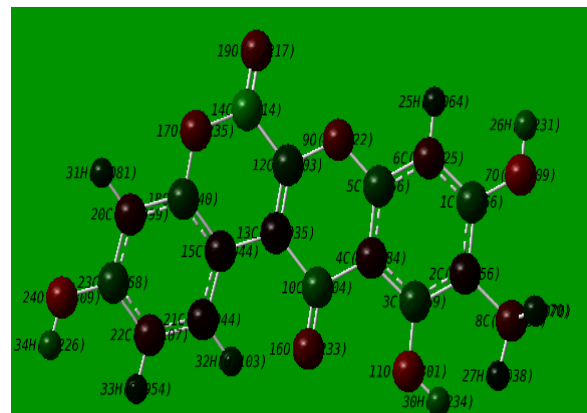
Boeravinone D Homo



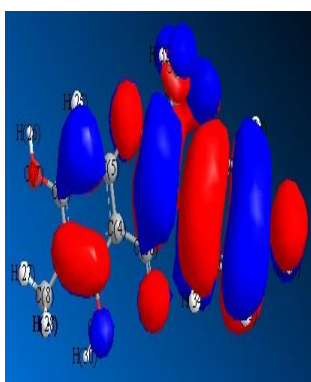
Boeravinone D Lumo



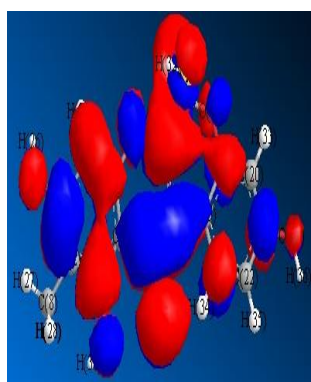
Boeravinone E Optimised



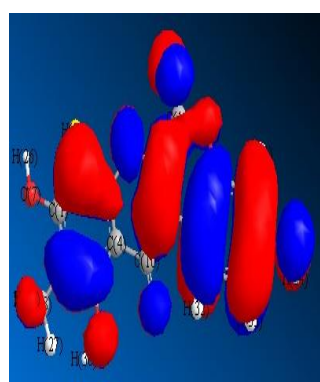
Boeravinone F Optimised



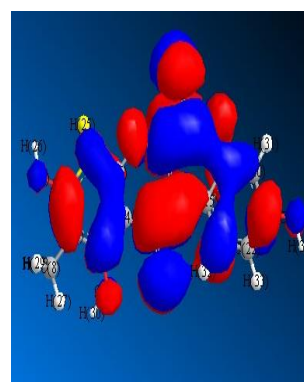
Boeravinone E Homo



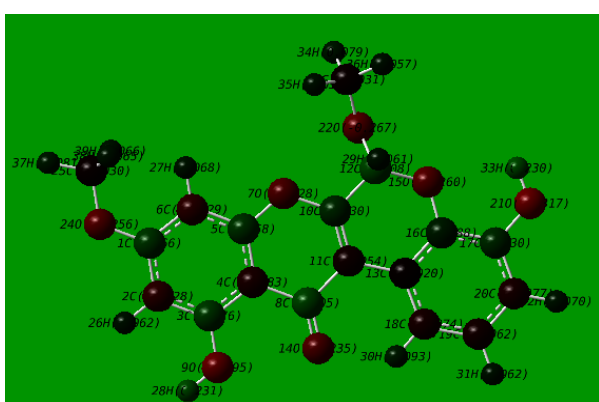
Boeravinone E Lumo



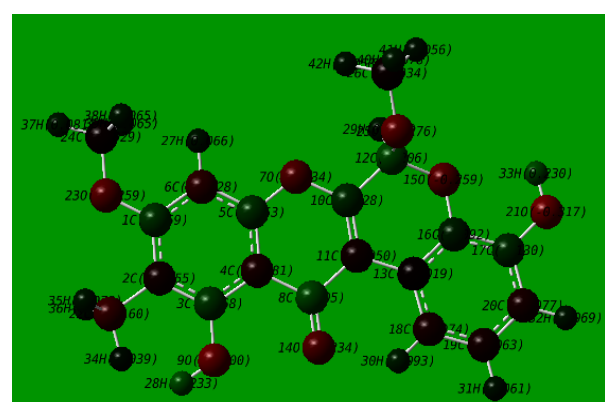
Boeravinone F Homo



Boeravinone F Lumo



Boeravinone G Optimised



Boeravinone H Optimised

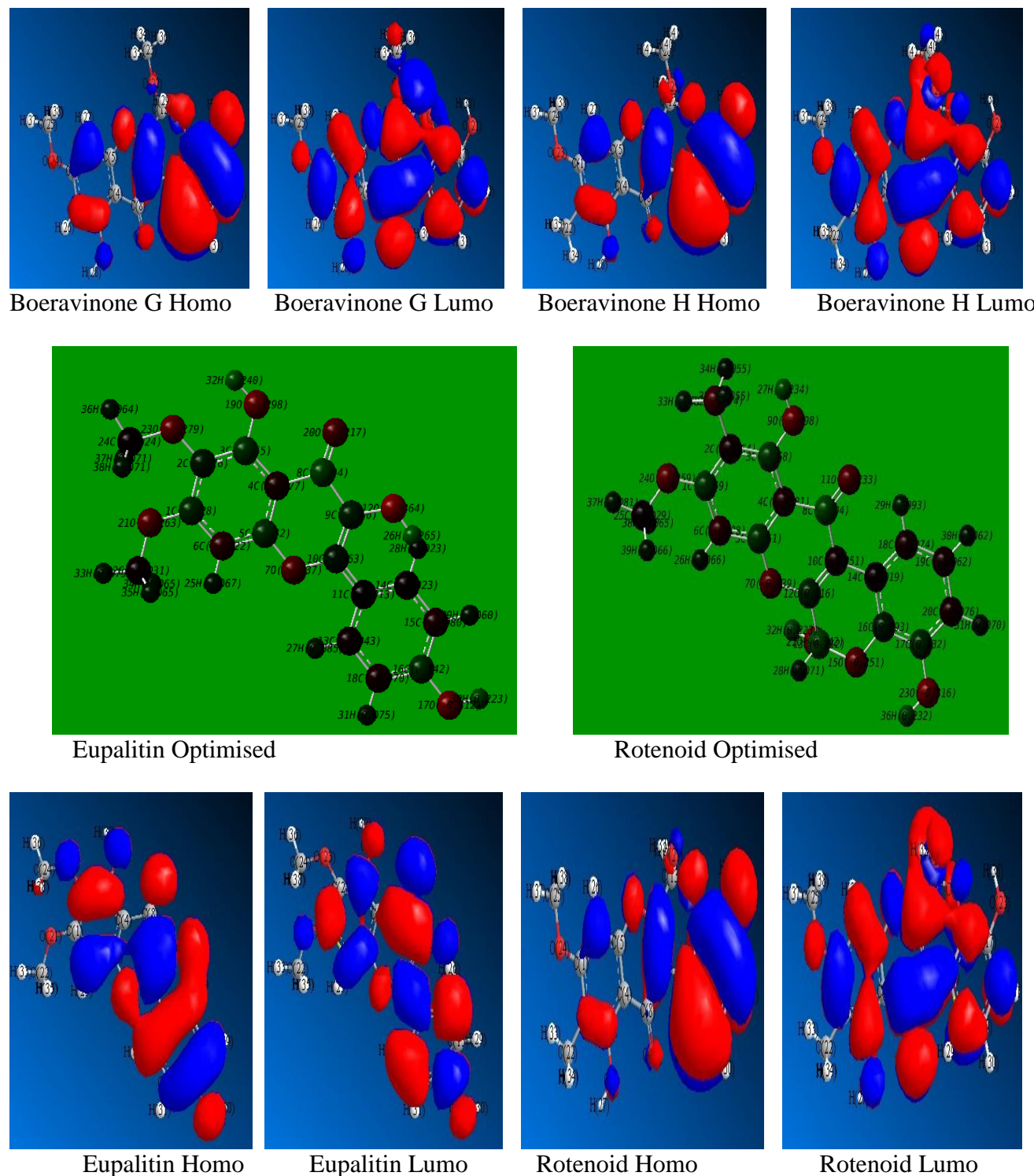


Figure 7. Optimized molecular structure with mulliken charges of the active constituents of Punarnava (*Boerhavia diffusa*) extract and the frontier molecular orbital density distribution (a) HOMO (b) LUMO

The lower the value of E_{LUMO} , the more probable it is that the molecule would accept electrons [26]. As for the values of ΔE ($E_{\text{LUMO}} - E_{\text{HOMO}}$) concern; lower values of the energy difference ΔE will cause higher inhibition efficiency because the energy to remove an electron from the last occupied

orbital will be low [27]. For the dipole moment (μ), higher values of μ will favor strong interaction of the inhibitor molecules with metal surface and lower values favor the accumulation of inhibitor molecules around electrode surface [28]. Quantum chemical parameters presented in Table 4 confirmed good inhibition performance of active constituents of Punarnava extract as corrosion inhibitor and also confirmed strong interaction of Punarnava extract molecules with the metal surface and thereby forming protective adsorption layer at mild steel/acid solution interface.

Table 4. Calculated Quantum chemical parameters of studied inhibitor

Active Constituents	HOMO (Hartree)	LUMO (Hartree)	ΔE (LUMO-HOMO) (Hartree)	Dipole Moment (μ)	Molecular Volume (bohr**3/mol)
Boeravinone B	-0.29953	0.07376	0.37329	6.3371	2287.977
Boeravinone C	-0.31202	0.07506	0.38708	5.5824	2444.095
Coccineone B	-0.30187	0.07191	0.37378	5.7762	2146.942
Boeravinone D	-0.32701	0.08336	0.41037	2.1127	2536.409
Boeravinone E	-0.29028	0.07411	0.36439	6.5844	2191.729
Boeravinone F	-0.31006	0.03429	0.34435	5.5200	2282.542
Boeravinone G	-0.29949	0.07388	0.37337	7.5052	2604.153
Boeravinone H	-0.29431	0.07704	0.37135	8.5108	2901.058
Eupalitin	-0.28869	0.06584	0.35453	7.4980	2676.698
Rotenoid	-0.29719	0.07166	0.36885	8.6636	2483.711

4. MECHANISM OF INHIBITION

Inhibition performance of Punarnava (*Boerhavia diffusa*) extract for mild steel in 1 M HCl interface depends on the extent of adsorption and adsorption depends on several factors such as the number of adsorption sites, molecular size, and mode of interaction with the metal surface and extent of formation of metallic complexes. The neutral molecules may be adsorbed on the mild steel surface through the chemisorption mechanism, involving the displacement of water molecules from the mild steel surface and the sharing electrons between the hetero atoms and iron. The inhibitor molecules can also adsorb on the mild steel surface on the basis of donor-acceptor interactions between π -electrons of the aromatic ring and vacant d-orbitals of surface iron atoms [29-31].

It is not possible to consider a single adsorption mode between inhibitor and metal surface because of the complex nature of adsorption and inhibition of a given inhibitor. There may be synergism between Punarnava (*Boerhavia diffusa*) extract and the mild steel surface due to large number of active constituents present in the extract. Also, the adsorbed active constituents may cover the active sites due to their large molecular volume on the mild steel surface reducing the corrosion. Thus, we can assume that inhibition of mild steel corrosion in 1 M HCl is due to the adsorption of extract constituents on the mild steel surface.

5. CONCLUSIONS

1. The inhibitor studied has an excellent inhibition effect for the corrosion of mild steel in 1 M HCl. The high inhibition efficiencies of were attributed to the adherent adsorption of the inhibitor molecules on the mild steel surface.
2. The adsorption of these compounds on the mild steel surface obeyed the Langmuir adsorption isotherm.
3. Potentiodynamic polarization studies revealed that the studied inhibitor is mixed type inhibitor.
4. The values of the obtained double layer capacitance (C_{dl}) have shown a tendency to decrease, which can result from a decrease in local dielectric constant and/or an increase in thickness of the electrical double layer.
5. Quantum chemical approach is adequately sufficient to predict the structure and molecule suitability to be an inhibitor.

References

1. I.B. Obot, E.E. Ebenso, Zuhair M. Gasem, *Int. J. Electrochem. Sci.* 7 (2012) 1997.
2. Nnabuk O. Eddy, Femi E. Awe, Abdulfatai A. Siaka, Ladan Magaji, Eno E. Ebenso, *Int. J. Electrochem. Sci.* 6 (2011) 4316.
3. E.E. Oguzie, C.K. Enenebeaku, C.O. Akalezi, S.C. Okoro, A.A. Ayuk, E.N. Ejike, *J.Coll. Inter.Sci.* 349 (2010) 283.
4. Ambrish Singh, I. Ahamad, D. K. Yadav, V. K. Singh, M. A. Quraishi, *Chem. Engg. Comm.* 199 (2012) 63.
5. Husnu Gerengi, Halil Ibrahim Sahin, *Ind. Eng. Chem. Res.* 51 (2012) 780.
6. Ambrish Singh, I Ahamad, V. K. Singh, M. A. Quraishi, *J. Solid State Electrochem.* 5 (2011) 1087.
7. M.A. Quraishi, Ambrish Singh, V. K. Singh, D. K. Yadav, A. K. Singh, *Mater. Chem. Phys.* 122 (2010) 114.
8. M. Lebrini, F. Robert, A. Lecante, C. Roos, *Corros. Sci.* 53 (2011) 687.
9. Ambrish Singh, M. A. Quraishi, *Res. J.Rec. Sci.* 1 (2012) 57.
10. A. Lecante, F. Robert, P.A. Blandinières, C. Roos, *Cur. Appl. Phys.* 11 (2011) 714.
11. Ambrish Singh, V. K. Singh, M. A. Quraishi, *Intern. J. Corros.* (2010) doi:10.1155/2010/275983.
12. Ambrish Singh, V. K. Singh, M. A. Quraishi, *Rasayan J. Chem.* 3 (2010) 811.
13. Ambrish Singh, Eno E. Ebenso, M.A. Quraishi, *Int. J. Electrochem. Sci.* 7 (2012) 3409.
14. Ambrish Singh, I. Ahamad, M. A. Quraishi, *Arab. J. Chem.* doi10.1016/j.arabjc.2012. 04. 029.
15. Ambrish Singh, M. A. Quraishi, *Intern. J. Corros.* doi:10.1155/2012/897430.
16. Kuldeep Rajpoot, R. N. Mishra, *Intern. J. Res. Pharm. Biom. Sci.* 2 (2011) 1451.
17. Anil kumar et al, *I.J.R.R.P.A.S.* 2 (2009) 347.
18. Natasa Milic, PhD Thesis, Faculty of Pharmacy, Department of Experimental Pharmacology, University of Naples, 2007.
19. Gaussian 03, Revision E.01, Frisch, M.J.; Trucks, G.W.; Schlegel, H.B.; Scuseria, G.E.; Robb, M.A.; Cheeseman, J.R.; Montgomery, Jr. J.A.; Vreven, T.; Kudin, K.N.; Burant, J.C.; Millam, J.M.; Iyengar, S.S.; Tomasi, J.; Barone, V.; Mennucci, B.; Cossi, M.; Scalmani, G.; Rega, N.; Petersson, G.A.; Nakatsuji, H.; Hada, M.; Ehara, M.; Toyota, K.; Fukuda, R.; Hasegawa, J.; Ishida, M.; Nakajima, T.; Honda, Y.; Kitao, O.; Nakai, H.; Klene, M.; Li, X.; Knox, J.E.; Hratchian, H.P.; Cross, J.B.; Bakken, V.; Adamo, C.; Jaramillo, J.; Gomperts, R.; Stratman, R.E.; Yazyev, O.;

- Austin, A.J.; Cammi, R.; Pomelli, C.; Ochterski, J.W.; Ayala, P.Y.; Morokuma, K.; Voth, G.A.; Salvador, P.; Dannenberg, J.J.; Zakrzewski, V.G.; Dapprich, S.; Daniels, A.D.; Strain, M.C.; Farkas, O.; Malick, D.K.; Rabuck, A.D.; Raghavachari, K.; Foresman, J.B.; Ortiz, J.V.; Cui, Q.; Baboul, A.G.; Clifford, S.; Cioslowski, J.; Stefanov, B.B.; Liu, G.; Liashenko, Piskorz, A. P.; Komaromi, I.; Martin, R.L.; Fox, D.J.; Keith, T.; Al-Laham, M.A.; Peng, C.Y.; Nanayakkara, A.; Challacombe, M.; Gill, P.M.W.; Johnson, B.; Chen, W.; Wong, M.W.; Gonzalez, C.; Pople, J.A.; Gaussian, Inc., Wallingford CT, 2007.
20. I. Ahamad, R. Prasad, M. A. Quraishi, *Corros. Sci.* 52 (2010) 3033.
 21. K. Juttner, *Electrochim. Acta*. 35 (1990) 1501.
 22. N. O. Eddy, S. R. Stoyanov, Eno E. Ebenso, *Int. J. Electrochem. Sci.* 5 (2010) 1127.
 23. Ambrish Singh, Eno E. Ebenso, M.A. Quraishi, *Int. J. Electrochem. Sci.* 7 (2012) 4766.
 24. I. Lukovits, E. Kalman, F. Zucchi, *Corros.* 57 (2001) 3.
 25. I. Ahamad, R. Prasad, M.A. Quraishi, *Corros. Sci.* 52 (2010) 1472.
 26. J. Fang, J. Li, *J. Mol. Struct. (Theochem)* 593 (2002) 179.
 27. P. Zhao, Q. Liang, Y. Li, *Appl. Surf. Sci.* 252 (2005) 1596.
 28. D. K. Yadav, M.A. Quraishi, B. Maiti, *Corros. Sci.* 55(2011) 254.
 29. R. S. Goncalves, D. S. Azambuja, A. M. Serpa Lucho, *Corros. Sci.* 44 (2002) 467.
 30. G. N. Mu, T. P. Zhao, M. Liu, T. Gu, *Corros.* 52 (1996) 853.
 31. M.A. Quraishi, M.Z.A. Rafiquee, S. Khan, N. Saxena, *J. Appl. Electrochem.* 37 (2007) 1153.